Short Range Order of Rodlike Polyelectrolytes in the Isotropic Phase

Valeria Castelletto[†,§] and Lia Q. Amaral[*,‡]

Laboratório Nacional de Luz Síncrotron, Caixa Postal 6192, CEP 13083-970, Campinas, SP, Brazil, and Instituto de Física, Universidade de São Paulo, Caixa Postal 66318, CEP 05315-970, São Paulo, SP, Brazil

Received November 3, 1997; Revised Manuscript Received January 20, 1999

ABSTRACT: The local order of aqueous solutions of rodlike polyelectrolytes is analyzed. It is shown that the scaling of the full width at half-height of the first peak of the static structure factor with the concentration C of polyelectrolyte is similar to the scaling of the peak position of the first maximum: it changes from $C^{1/3}$ to $C^{1/2}$ as C varies from the dilute to the semidilute regime. This result enables us to estimate the number of ordered next neighbor shells, N, arranged locally around a central particle. It is shown, in good agreement with Monte Carlo results, that $N \sim 1$ when the ionic strength of the solution, I, is $\sim 10^{-7}-10^{-5}$ M and the polyelectrolyte surface charge in the solution, Q, is on the order of hundreds of electrons. This order decreases when I goes to $\sim 10^{-3}-10^{-2}$ M and Q decreases by 1 order of magnitude.

1. Introduction

There are many experimental and theoretical studies of the static structure factor, $S(q)$, corresponding to salt-free and salt-containing aqueous solutions of cylindrical polyelectrolytes in the isotropic phase.[1−10] The $S(q)$ functions obtained from all these works show a first peak at small scattering angles, which varies with the concentration C of polyelectrolyte.

The local order of these solutions depends on the ionic strength of the solution, I, and on the surface charge of the polyelectrolyte in the solution, Q. Variations in these two factors are directly related to changes in the first peak of $S(q)$.[6]

The $S(q)$ function of these systems depends on the relative position of the center of mass of the particles, as well as on the orientation of each particle.[6−10] In the isotropic phase, the variation of the angular position of the first peak of $S(q)$, q_m, with the polyelectrolyte concentration of the sample C changes from $C^{1/3}$ to $C^{1/2}$, when the system goes from the dilute ($C < C^*$; C^* = critical concentration of the system = [1 polyelectrolyte/L^3], L being the polyelectrolyte length) to the semidilute regime ($C > C^*$). This is an experimental evidence of how the anisotropic particle shape affects the interaction between the polyelectrolyte molecules, and has been explained by invoking the stronger influence of the angular correlations in the semidilute regime than in the dilute regime, in the expansion of $S(q)$ in rotational invariants.[9,10]

The description of short-range order in a polyelectrolyte solution involves the mean nearest neighbor distance between the objects, s_0^{-1} ($s_0 = q_m/2\pi$), as well as the correlation length, ξ, both of them related to the $S(q)$ function.[1,2]

In a previous work we have shown that ξ in a semidilute solution of rodlike polyelectrolytes is slightly greater than the distance to the first neighbors. We reached this conclusion by testing simple models of the $S(q)$ functions of semidilute aqueous solutions against data from the literature.[1] Q and I values were not varied in our analysis.

In this work, we are reconsidering the interpretation given by us[1] to calculate ξ for solutions of rodlike particles. We will study the dependence of ξ on I and Q in the semidilute regime, restricting our study to small variations of I, i.e., to those related to the counterions contributions for salt-free solutions.

In our analysis, we will extend the comparison we have begun in our previous work to data from literature: we will use our $S(q)$ functions of the fragmented DNA aqueous solutions, already presented in that work,[1] and $S(q)$ functions, scanned from the literature, corresponding to aqueous solutions of fd-virus and tobacco mosaic virus (TMV).[4−6,9−10]

2. Results

In our analysis, $S(q)$ functions corresponding to six sets of theoretical and experimental results will be used. The name of each set of results, the samples used to obtain these results, the regime of these samples, and the class of result (theoretical or experimental) are specified in Table 1.

$S(q)$ curves of AM1 set (DNA) have been presented by us in a previous work[1] whereas $S(q)$ curves of AM2−AM5 sets are from virus solutions (taken from the literature).

$S(q)$ belonging to AM6−AM7 sets have been calculated by the Monte Carlo method, using a screened Coulomb potential to describe the interactions between the polyelectrolytes.[9,10]

The first peak of the static structure factors belonging to AM1−AM7 sets has been modeled with Gaussian and Lorentzian shapes. Figure 1 exemplifies the typical modeling obtained for all the $S(q)$ functions: as it has been previously discussed by us,[1] the best fitting was obtained using Gaussian functions.

The values of the full width at half-height of the Gaussian functions used to model the first peak on $S(q)$, $[\beta]_g$, are listed in Table 2. These values, multiplied by L, are shown in Figure 2 as a function of C/C^*.

Our results show that the dependence of $[\beta]_g$ on C also presents a power law behavior. From Figure 2, it is possible to observe that $[\beta]_g$ also depends on some other

† Laboratório Nacional de Luz Síncrotron.
‡ Universidade de São Paulo.
§ Present address: Laboratoire Léon Brillouin, CEA-CNRS, Saclay, F-91191 Gif-sur-Yvette Cédex, France.

10.1021/ma971617c CCC: $18.00
Published on Web 04/22/1999

Table 1. Names of the Sets of $S(q)$ Functions used in This Work, Systems to Which They Belong, Regimes of the System, and Classes of Results[a]

set	system	regime of the system	class of result
AM1	DNA/water	semidilute	experimental[1]
AM2	TMV virus/water	semidilute	experimental[6]
AM3	fd-virus/water	semidilute	experimental[5]
AM4	fd-virus/water/ /ion exchange resin	semidilute	experimental[5,10]
AM5	TMV virus/water/ /ion exchange resin	dilute	experimental[4]
AM6	fd-virus/water/ /ion exchange resin	dilute/ semidilute	theoretical[10] (fitted charge)
AM7	TMV virus/water/ /ion exchange resin	dilute/ semidilute	theoretical [9] (constant charge)

[a] $S(q)$ functions of AM1 set were presented in ref 1; $S(q)$ functions of the AM3 set were used for Figure 11 of ref 1.

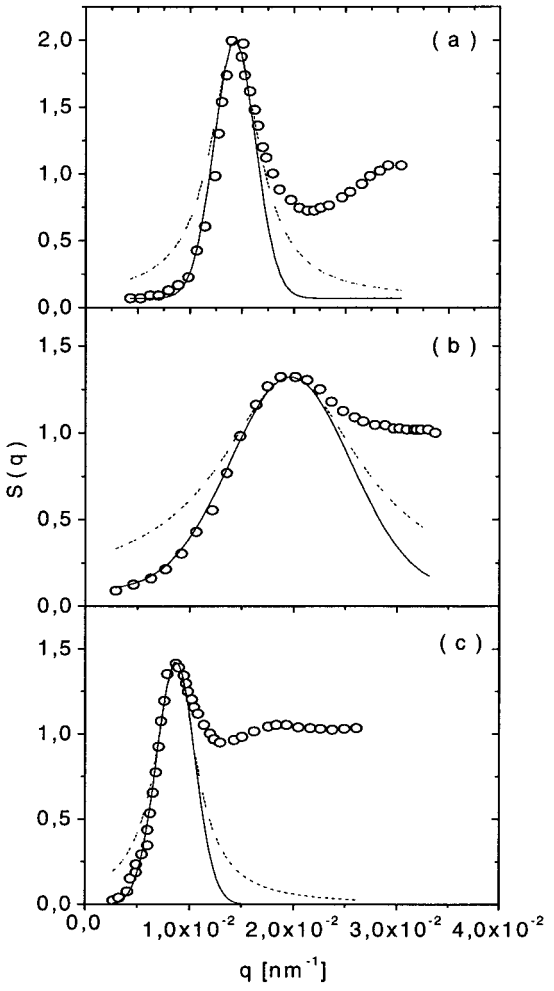

Figure 1. (○) Static structure function $S(q)$; (—) modeling with a Gaussian function; (- -) modeling with a Lorentzian function: (a) AM4 set, 0.128 g/L; (b) AM3 set, 0.184 g/L, and (c) AM7 set, 0.123 g/L.

parameters besides C. It is also possible to observe that the theoretical AM7 values (calculated for a constant charge) present a continuous transition at $C/C^* = 1$, while the experimental sets AM4 and AM5 seem to indicate a discontinuity at $C/C^* = 1$. Then, our results are consistent with three curves with exponent 1/2 in the semidilute regime, and two curves with exponent 1/3 in the dilute regime. This behavior can be summed up in a general formula

$$L[\beta]_g = A(C/C^*)^x \qquad (1)$$

Table 2. Parameters Values Obtained from the Modeling of the First Peak in the Structure Factor Function Curves Belonging to AM1−AM7 Sets Using a Gaussian Function: Concentration of the Sample C, Critical Concentration C^*, C/C^* Fraction, Gaussian Full Width at Half-Height $[\beta]_g$ and Polyelectrolyte Length L

	C [g/L]	C^* [g/L]	C/C^*	$[\beta]_g$ [1/nm]	L [nm]
AM1[1]	20	4	5	0.52	34
	40		10	0.64	
	60		15	0.89	
	80		20	0.68	
	100		25	0.85	
	146		36.5	0.92	
	202		50.5	1.01	
AM2[6]	14.3	2.45	5.84	0.0612	300
	21.8		8.898	0.0706	
	26.7		10.898	0.0542	
AM3[5]	0.059	0.04	1.475	0.0094	880
	0.097		2.425	0.0106	
	0.184		4.6	0.0141	
	0.275		6.875	0.0177	
	0.375		9.375	0.0188	
AM4[5,10]	0.051	0.04	1.275	0.0040	880
	0.091		2.275	0.0049	
	0.128		3.2	0.0036	
	0.163		4.075	0.0059	
	0.238		5.95	0.0075	
	0.33		8.25	0.0089	
	0.564		14.1	0.0141	
AM5[4]	0.11	2.45	0.045	0.0031	300
	0.27		0.11	0.0035	
	0.43		0.176	0.0042	
	1.05		0.428	0.0052	
	2.07		0.845	0.0094	
AM6[10]	0.021	0.04	0.52	0.0024	880
	0.06		1.51	0.0036	
AM7[9]	0.123	2.45	0.05	0.0043	300
	1.225		0.5	0.0086	
	2.45		1	0.0118	
	9.8		4	0.0236	

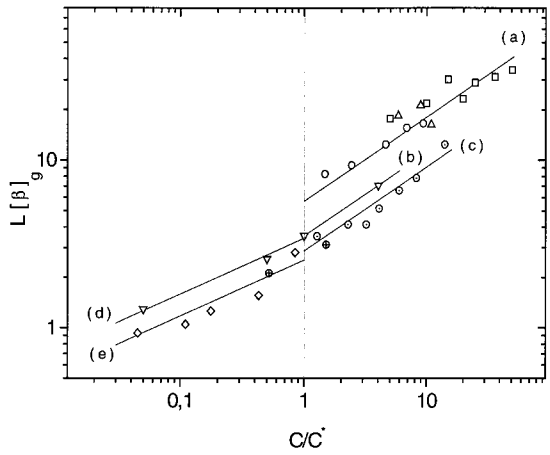

Figure 2. Dependence of $[\beta]_g$ with C/C^*. Results were obtained from the modeling of the first peak of $S(q)$ functions of the different sets of samples: (□) AM1; (△) AM2; (○) AM3; (⊙) AM4; (◇) AM5; (⊕) AM6; (▽) AM7. Fitting from eq 1: (a) $A = 5.69 \pm 0.26$, $x = 1/2$; (b) $A = 3.54 \pm 0.09$, $x = 1/2$; (c) $A = 2.88 \pm 0.13$, $x = 1/2$; (d) $A = 3.43 \pm 0.1$, $x = 1/3$; (e) $A = 2.54 \pm 0.16$, $x = 1/3$.

where A and x values, corresponding to each fitting, are listed in Table 3. Important shifts of q_m are observed only with addition of salt, which leads to large variations in the ionic strength.[6] As is well-known, the positions of the first peak of $S(q)$ for AM1−AM4 and AM6−AM7

Table 3. Data Related to the Fitting Through Eq 1: Set of Data, Equation Coefficient *A*, Equation Exponent *x*, Estimated Ionic Strength of the Data Set Solutions *I*, Surface Charge of the Polyelectrolyte in the Solution *Q*, and Number of Next-Neighbor Shells *N* Obtained through the Evaluation of Eq 7 (the Notation *O*(*X*) Refers to the Order of the Magnitude *X*)

set	*A*	*x*	*I* [M]	*Q* [$\bar{e}$]	*N*
AM1−AM3	5.69 ± 0.26	1/2	$\sim10^{-3}$−10^{-2}	O (10)	0.58 ± 0.03
AM4, AM6	2.85 ± 0.16	1/2	$\sim10^{-7}$−10^{-5}	O (100)	1.15 ± 0.06
AM7	3.54 ± 0.09	1/2	$\sim10^{-7}$−10^{-5}	O (100)	0.93 ± 0.02
AM5−AM6	2.54 ± 0.16	1/3	$\sim10^{-7}$−10^{-5}	O (100)	1.28 ± 0.08
AM7	3.43 ± 0.1	1/3	$\sim10^{-7}$−10^{-5}	O (100)	0.94 ± 0.03

sets in the semidilute regime, are fitted by[4−6,9−10]

$$q_m L = 7.0(C/C^*)^{1/2} \quad (2)$$

On the other hand, q_m values for AM5−AM7 sets in the dilute regime are fitted by[4,6]

$$q_m L = 6.9(C/C^*)^{1/3} \quad (3)$$

Comparison of eqs 1, 2, and 3 shows that $[\beta]_g$ is proportional to q_m. A plot of the relative width $\Delta q/q_m$ as a function of concentration was made in a previous publication (Figure 3 of ref 10), but no conclusions were explicitly drawn about an universal power law.

The scaling behavior evidenced in Figure 2 means that the concept of an "effective" correlation length holds for these rod systems.

It is well-known that for a monatomic fluid, in which each particle position is completely defined by three coordinates, the pair correlation function of the system decays exponentially with r.[2,11] Consequently, the interference function of the system takes a Lorentzian shape, and the correlation length is inversely proportional to the full width at half-height of the Lorentzian function, $[\beta]_l$.

In our work, we have empirically determined that the first peak of $S(q)$ has a Gaussian shape. $[\beta]_g$ is related to the local order of the system, since it represents a measure of the width of the first peak of $S(q)$. As already mentioned above, ξ is well-defined for $S(q)$ with a Lorentzian shape. Thus, to find an expression for ξ as a function of $[\beta]_g$ for a rodlike polyelectrolyte solution, we constrained the area under the Gaussian function fitting the first peak of $S(q)$ to be equal to the area under a Lorentzian $S(q)$ function. Since the system is isotropic, this condition can be stated in the one-dimensional projection of the intensity curve:

$$\int_{-\infty}^{\infty} \frac{dq}{1 + (2q/[\beta]_l)^2} = \int_{-\infty}^{\infty} \exp(-2.8q^2/[\beta]_g)\, dq \quad (4)$$

With eq 4, the divergence of the left-hand side of the three-dimensional integral is avoided without the necessity of introducing specific limits for the integration. Such limits are not physically meaningful since the intensity curve can be cut at the background level. It results in

$$\xi = \frac{2.95}{[\beta]_g} \quad (5)$$

where ξ now measures the local order in the rodlike polyelectrolyte system.

This attempt to calculate ξ is more realistic than that proposed by us in a previous work.[1] In that work, we used the correlation length corresponding to a monatomic fluid, replacing $[\beta]_l$ by $[\beta]_g$: however, we erroneously introduced a π factor (eq 11 of ref 1). In fact the criterion $[\beta]_l = [\beta]_g$ should lead to a correlation length $\sim^2/_3$ smaller than the present criterion of equal areas for the Gaussian and the Lorentzian functions, instead of leading to a factor of 2 larger as would be expected from eq 11 of ref 1.

It is also interesting to compare these criteria with the value obtained from the well-known Debye−Scherrer formula[12] which relates the width of a diffraction peak with the size L_c of the crystallite, and gives

$$L_c = \frac{5.65}{[\beta]_g} \quad (6)$$

Such size is almost twice the correlation length of eq 5, and that is understandable, since the correlation length measures the neighbors from a central object, while L_c measures the total range of correlation. If the exponent in eq 1 is equal to that in eqs 2 or 3, it is possible to calculate ξ by using eq 5:

$$\xi = \left(\frac{B}{A}\right)\left(\frac{2.95}{2\pi}\right)s_0^{-1} = Ns_0^{-1} \quad (7)$$

Here B is equal to 7.0 or 6.9 depending on whether eq 2 or eq 3 has been used. Equation 7 defines the length of correlation as the number N of next neighbor shells times the mean distance between them.

To have more confidence in the proposed criteria of equal areas (eq 4) we have calculated N from eq 7, using $S(q)$ functions from numerical Monte Carlo results (AM6−AM7 sets). These calculations[9] (Tables 1 and 2 and Figure 2), have shown that at all concentrations the local order is confined essentially to a first neighbor shell. In particular at $C/C^* = 4$ the merely positional order gets lost and the orientational order of nearest neighbors becomes important (there is a tendency of parallel ordering of nearest neighbors).

Our calculation of ξ corresponding to AM7 set (Table 3) shows that there is an approximately first neighbor local order in the solution, in good agreement with Monte Carlo calculations mentioned in the paragraph above.

N was determined for all AM1-AM7 sets using eq 7. Results are listed in Table 3.

2.1. Dependence of $[\beta]_g$ on the Parameters of the Solution. Equation 5 shows that $[\beta]_g$ is associated with the local order of the system. Besides this, it depends on both I and Q. We have already mentioned that the ionic strength of the solution and the surface charge of the polyelectrolyte in the solution will be chosen as relevant parameters of our analysis to explain the physical meaning of results in Table 3. Therefore, it is necessary to determine their values for each set in Table 1. I is defined according to

$$I = 1/2\sum \phi_i Z_i^2 \quad (8)$$

where ϕ_i is the concentration of counterions of the ith class and Z_i is the charge of each counterion, while Q for monovalent counterions is given by

$$Q = \frac{N_i}{N_p}\bar{e} \tag{9}$$

where N_i is the number of counterions in the solution, N_p is the number of particles in the solution and $\bar{e} = 1.6 \times 10^{-19}$ C is the charge of one electron.

Q differs from the total superficial polyelectrolyte charge: this last value is well-known to be $\sim 202\bar{e}$, $\sim 10000\bar{e}$, and $\sim 1000\bar{e}$, for DNA ($L = 34$ nm),[13] fd-virus ($L = 880$ nm),[5] and TMV virus ($L = 300$ nm)[4] respectively.

2.2. Estimation of The Ionic Strength of the Solution and of the Superficial Charge of the Polyelectrolytes in the Solution. 2.2.1. AM1 Set. The counterions accumulation near the surface of a charged polyelectrolyte in the solution leads to a "charge condensation" effect:[3,14] a fraction of the counterions are "territorially" bound to the polyelectrolyte, while the rest remain free in a Debye−Hückel cloud around the polyelectrolyte. "Territorially" bound counterions neutralize the equivalent units of the groups on the surface of the polyelectrolyte and this effect leads to a Q value smaller than the total charge of the polyelectrolyte surface. If a solution of cylindrical polyelectrolytes with monovalent counterions satisfies[3,14]

$$ZL_B > 1 \tag{10}$$

where $Z =$ [total surface charge of the polyelectrolyte/L] and $L_B =$ Bjerrum length 7.1 Å, the condensation charge theory establishes that a fraction $(1 - 1/Zl_B)$ of the polyelectrolyte are neutralized by "territorially" bound counterions, whereas a fraction, $1/ZL_B$, of the counterions remain free in the solution.

From this result it is possible to calculate the number of both free and condensed counterions present in the solution and their contribution to the ionic strength, using eq 8.

The ionic strength of the AM1 set will be calculated as the one resulting from the DNA Na^+ present in the solution due to the "charge condensation" effect.

For fragmented DNA 34 nm long, $ZL_B = 4.19$. Thus, 76% of the DNA surface charge will be neutralized by the Na^+ "territorially" bound counterions. The free counterions (24%) contribute to the ionic strength of the solution.

Table 4 lists the value of I due to the contribution of the Na^+ free counterions calculated according to eq 8 for each C. It is possible to conclude that $I \sim 10^{-3} - 10^{-2}$ M. The 76% of the DNA charge neutralized by the Na^+ counterions corresponds to $Q = 48\bar{e}$.

The radius of the Debye−Hückel cloud around the polyelectrolyte made by the free counterions $k^{-1} = (0.0151L_BI)^{-1/2}$ can be calculated by using data listed in Table 4. The result is that the ratio of k^{-1} (Debye length) to the distance between first neighbors (calculated from q_m of our DNA $S(q)$ curves[1]) varies from 2.7 to 3.2 over the wide concentration range of the AM1 set. Therefore, there is always enough space for condensation within a first neighbor shell.

2.2.2. AM2-AM7 Sets. TMV and fd-virus have ionic carboxyl groups on their surface. These groups, in aqueous solution, produce H_3O groups which are the counterions of these polyelectrolytes. Due to the distance between these ionic groups, the "condensation charge" effect does not take place.[15] It is not possible to determine with precision the effective charge of each virus, because the degree of the counterions dissociation depends on the pH of the solution.

An ion-exchange resin is usually added to the solutions of TMV and fd virus, to attain the minimum value of the ionic strength of the solution. The function of the resin consists of removing the impurities from the solution. Under these conditions, it has been established that the counterions dissociation leads to a Q value of a few hundreds of $\bar{e}$, for concentrations close to C^*. If the ion-exchange resin is not added to the solution, the ionic strength of the solution is increased by the CO_2 absorption during the sample preparation.

Although the CO_2 contribution to the solution ionic strength is extremely low, it neutralizes a fraction of the polyelectrolyte surface charge.[15] The experimental manifestation of this effect is a strong narrowing of the first peak of the $S(q)$ function, for a determined C value, when the ion-exchange resin is added to the solution.[15]

According to the paragraph above, Q values for AM4-AM5 sets were estimated in the literature as hundreds of $\bar{e}$, and I, completely due to the dissociated counterions, was estimated as $I \sim 10^{-6}$ M.

The ionic strength used in the Monte Carlo calculations (AM6−AM7 sets) was calculated according to eq 8, considering only the contribution of the counterions dissociated from the polyelectrolytes.[9,10]

For the AM6 set $Q = 408\ \bar{e}$ was used for 0.021 g/L and $Q = 360\bar{e}$ was used for 0.06 g/L. According to eq 8, this corresponds to $I \sim 10^{-7}$ M for the more dilute sample and to $I \sim 10^{-6}$ M for the more concentrated one.

$Q = 150\bar{e}$ was used for the AM7 set: eq 8 gives $I \sim 10^{-7}$ M for 0.123 g/L, $I \sim 10^{-6}$ M for 1.225 g/L, and $I \sim 10^{-5}$ M for 9.8 g/L.

3. Conclusions

Our results show that the scaling of the full width at half-height of the first peak of $S(q)$, corresponding to a solution of rodlike polyelectrolytes, with C, changes from $C^{1/3}$ to $C^{1/2}$ when C goes from the dilute to the semidilute regime. This behavior is similar to that previously reported in the literature for q_m.[3−10]

The peak position q_m is weakly affected by variations of the ionic strength for salt-free solutions. In this work it is shown that this does not happen with the full width at half-height of the first peak on $S(q)$: a clear evidence of the influence of I on the local order of the solution and of the agreement between experimental and theoretical results is shown in Figure 2 (and summarized in Table 3), as will be discussed below.

It is necessary to clarify that the set of numbers given for N in Table 3 does not mean "exact absolute values" at all, but the set is meaningful for comparative and relative purposes. $[\beta]_g$ is very sensitive even to a small variation in I; in terms of our analysis this means that although fitting through eq 1 is satisfactory (Figure 2), not all the plotted points are on the fitting curve. Moreover, the criterion of equal areas leading to eqs 4 and 5 is somewhat arbitrary. Nevertheless, the scaling obtained (Figure 2) is sufficiently well defined in order to make the concept of N meaningful.

At the semidilute regime, the results for AM4−AM7 sets are fitted by eq 1 evaluated for $A = 2.88$ and 3.54, with $x = 1/2$. So, it can be inferred (Table 3) that eq 1 calculated for these values of A and x fits data corresponding to semidilute solutions with $I \sim 10^{-7} - 10^{-5}$ M and Q on the order of hundreds of $\bar{e}$ and that under these

Table 4. Ionic Strength of AM1 Samples Set: Sample Concentration *C* and Ionic Strength of the Solution *I* Calculated According to Eq 8

C [g/L]	20	40	60	80	100	146	202
I [M]	5.65×10^{-3}	1.13×10^{-2}	1.69×10^{-2}	2.25×10^{-2}	2.82×10^{-2}	4.12×10^{-2}	5.71×10^{-2}

conditions $N \sim 1$. Solutions with similar values of Q, I, and N are fitted at the dilute regime by eq 1 calculated for $A = 2.54$ and 3.43, with $x = {}^1/_3$.

Ion-exchange resin was not added to AM1−AM3 sets: according to what is expected, Table 2 and Figure 2 show that the value of $[\beta]_g$ for these sets is higher than for AM4 set (with ion-exchange resin). Results for AM1−AM3 sets are fitted by eq 1 for A = 5.69, with $x = {}^1/_2$. This suggests that I and Q values are similar for AM1−AM3 sets. Therefore, eq 1 calculated with A = 5.69, with $x = {}^1/_2$, fits the data corresponding to semidilute solutions with $I \sim 10^{-3}-10^{-2}$ M and Q in the order of tens of $\bar{e}$ (Table 3).

Q corresponding to AM2 and AM5 sets has been previously determined matching the height of the $S(q)$ function peak predicted by integral equation theory to the experimental data.[7] It has been concluded that Q is on the order of hundreds of electrons for AM5 and that it decreases to tens of electrons for AM2, in agreement with our results. Only the last point at $C = 10.84\ C^*$ shows a discrepancy since their fitted charge increases at this point. However, their estimated charge is in fact zero at this point, and therefore the discrepancy seems not to be meaningful. It has been admitted that the oscillation in the theoretical Q might be due to the variation of the peak height from different experiments at the same concentration.[7]

From Table 3 and Figure 2, it is possible to conclude that the increase in I is accompanied by a decrease of Q. This is experimentally manifested through a broadening of $[\beta]_g$ and leads to a decrease in N in the semidilute regime. In particular, considering the results related to experimental and theoretical data in the semidilute regime (AM1−AM4, AM6−AM7), when I goes from $\sim 10^{-7}-10^{-5}$ to $\sim 10^{-3}-10^{-2}$ M and Q decreases by 1 order of magnitude, the presence of a local order in the solution is practically lost, since it does not fully reach a first-neighbor shell.

It was also established that there is a local order slightly higher than a first-neighbor shell in the dilute regime for $\sim 10^{-7}-10^{-5}$ M and for Q in the order of hundreds of $\bar{e}$.

Figure 2 shows a particular result related to the sets containing theoretical $S(q)$ functions. Data from the AM7 set shows a continuous transition through $C/C^* = 1$, whereas data from the AM6 set follow the experimental results, which show a discontinuous transition. This is because, for the AM7 set, Q was fixed for all C values in order to calculate the $S(q)$ functions. Q is probably underestimated for the AM7 set, and since a repulsive Coulombian potential was used to describe the interactions between the polyelectrolytes in these calculations, the interaction between rods is weakened. This leads to a broadening of the $S(q)$ width, and the $[\beta]_g$ values for AM7 are larger than those for the AM6 set.

Acknowledgment. Financial support of the FINEP foundation is acknowledged. V. Castelletto had a CNPq doctoral fellowship and is grateful for a postdoctoral fellowship from the FAPESP. The authors would also like to thank C. V. Teixeira who kindly made the English revision of the manuscript.

References and Notes

(1) Castelletto, V.; Itri, R.; Amaral, L. Q.; Spada, G. P. *Macromolecules* **1995**, *28*, 8395.
(2) Geissler, E.; Horkay, F.; Hecht, A. M.; Rochas, C.; Lindner, P.; Bourgaux, C.; Couarraze, G. *Polymers* **1997**, *38*, 15.
(3) Wang, L.; Bloomfield, V. A. *Macromolecules* **1991**, *24*, 5791.
(4) Maier, E. E.; Schulz, S. F.; Weber, R. *Macromolecules* **1988**, *21*, 1544.
(5) Schulz, S. F.; Maier, E. E.; Weber, R. *J. Chem. Phys.* **1989**, *90*, 7.
(6) Maier, E. E.; Krause, R.; Deggelmann, M.; Hagenbüchle, M.; Weber, R.; Fraden, S. *Macromolecules* **1992**, *25*, 1125.
(7) Shew, C. Y.; Yethiraj, A. *J. Chem. Phys.* **1997**, *106*, 5706.
(8) Schneider, J.; Hess, W.; Klein, R. *Macromolecules* **1986**, *19*, 1729. Schneider, J.; Karrer, D.; Dhont, J. K. G. *J. Chem. Phys.* **1987**, *87*, 3008.
(9) Canessa, E.; D'Aguanno, B.; Weyerich, B.; Klein, R. *Mol. Phys.* **1991**, *73*, 175. Weyerich, B.; D'Aguanno, B.; Canessa, E.; Klein, R. *Faraday Discuss. Chem. Soc.* **1990**, *90*, 245.
(10) Hagenbüchle, M.; Weyerich, B.; Deggelmann, M.; Graf, R.; Krause, R.; Maier, E. E.; Schulz, S. F.; Klein, R.; Weber, R. *Physica A* **1990**, *169*, 29.
(11) Landau, L. D.; Lifshitz, E. M. *Statistical Physics*; Pergamon Press: Oxford, England, 1958.
(12) Cullity, B. D. *Elements of X-ray Diffraction*; Addison-Wesley: London, 1967.
(13) Lenhinger, A. L. *Principios de Bioquímica*; Sarvier: São Paulo, Brazil, 1985.
(14) Manning, G. S. *J. Chem. Phys.* **1969**, *51*, 934.
(15) Schulz, S. F.; Maier, E. E.; Krause, R.; Weber, R. *Prog. Colloid. Polym. Sci.* **1990**, *81*, 76. Schulz, S. F.; Maier, E. E.; Krause, R.; Hagenbüchle, M.; Deggelmann, M.; Weber, R. *J. Chem. Phys.* **1990**, *92*, 12. Schulz, S. F.; Maier, E. E.; Hagenbüchle, M.; Graf, C.; Weber, R. *Prog. Colloid. Polym. Sci.* **1991**, *84*, 356..

MA971617C